CHAPTER III

COMPONENTS CHARACTERIZATION AND MEASUREMENT METHODS

3.1 INTRODUCTION

In this chapter, the components characterization and two different measurement methods are presented. In Section 3.2, the basic experimental setup will be introduced. The different optical feedback schemes as shown in Chapter 4, 5 and 6 are based on this basic setup. Parameters of the components used in the setup are given in this chapter. Back reflections arising from the components are treated in Section 3.3. Different pumping schemes will be studied and compared in order to select the one that gives an acceptable performance. This is treated in Section 3.4. Since Time-Domain Extinction (TDE) Method are used for measuring the performance of the counter- and co-feedback schemes in the next two chapters, the principles of this measurement method will be described in Section 3.5. The results will be compared with that obtained from the conventional Interpolation Method. In the TDE method, the use of the additional instrument called Optical Amplifier Analyzer (OAA) introduces a high insertion loss to the input signal. Therefore, the input signal needs to be boosted up using another erbium-doped fiber amplifier (EDFA). A study will be carried out in Section 3.6 to investigate the boosted signal

that consists of the amplified spontaneous emission (ASE) contributed by the booster itself.

3.2 BASIC EXPERIMENTAL SETUP AND COMPONENTS CHARACTERIZATION

The experimental setup basically consists of a 980 nm pump source, an erbium-doped fiber (EDF), wavelength division multiplexers (WDM), couplers and isolators as shown in Fig. 3.1.

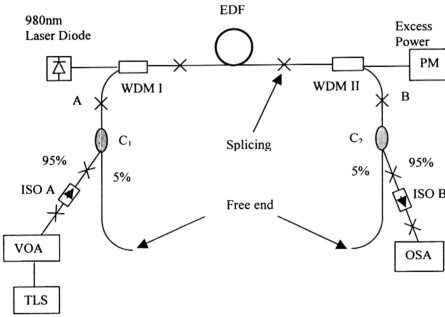

Fig. 3.1 *Basic experimental setup. (EDF: erbium-doped fiber; WDM: wavelength division multiplexer; PM: power meter; C: coupler; ISO: optical isolator; VOA: optical variable attenuator; TLS: tunable laser source; OSA: optical spectrum analyzer).*

It is a co-pumping scheme where the pump source and the injected signal are in the same direction. For the entire course of this study, three main different feedback-loops were formed based on this basic setup:

I. **Co-feedback:** An optical isolator was put in the optical path to form a unidirectional oscillation cavity in the direction of the injected signal. A wavelength selective element (tunable bandpass filter, in our case) was used to select the lasing wavelength of the oscillator.

II. **Counter-feedback:** The direction of the isolator was now reverse so that the oscillating laser was in the direction opposite that of the injected signal. The wavelength selective element was still applied.

III. **Regenerative-feedback:** In this scheme, the wavelength selective element was removed from the cavity to let the injected signal circulating in the cavity. Without the isolator, a bi-directional-feedback regenerative amplifier system was formed.

The components and materials used in the setup have been well characterized and they consist of:

1). **EDF:** The EDF used in the setup has a refractive index of 1.473, an Er^{3+} concentration of +440 ppm, a core radius of 1.68 μm and a length of 15 m.

2). **Pump source:** The pump source was from a 980 nm laser diode with the maximum output power of 134.5 mW. Fig. 3.2 shows the spectral profile with a resolution of 0.02 nm monitored from the 1 % port of a 980 nm coupler. The center wavelength of this pump source was 980.2 nm and the 3-dB spectral width was determined to be 0.1 nm.

3). **WDMs:** There were two WDMs in the system: one was to couple the pump source from the 980 nm port and the signal from the 1550 nm port to the EDF, and the other one was to couple out the excess pump and the amplified signal. The insertion loss (IL) for each WDM is shown in Fig. 3.3. Obviously, the ILs are not consistent over the measured wavelength range. The average IL is determined within the wavelength range from 1540 nm to 1560 nm, corresponding to the flat region in the ASE spectrum. Within this range, the IL is determined to be 0.39 dB for WDM I and 0.28 dB for WDM II.

4). **Couplers:** Both couplers, C_1 and C_2, were chosen to have the 95 % of input and output coupling ratio, respectively. This coupling ratio itself contributes to the degradation of the noise figure and signal gain as large as ~0.22 dB if the system is considered as a black box system. If a ratio of 90 % is chosen, the degradation will increase to be 0.46 dB. Fig. 3.4 shows the ILs for couplers C_1 and C_2 for the 95 % and 5 % ports.

5). **Optical Isolators:** ISO A and ISO B represent the isolators at the input and output ports, respectively. The ILs for both isolators are depicted in Fig. 3.5. The IL is determined to be 0.38 dB and 0.43 dB for ISO I and ISO II, respectively.

The WDMs, couplers and isolators were then spliced together and characterized again as a component. Fig. 3.6 shows the ILs for input and output ports. The IL for each port is lower than the sum of component's IL characterized individually due to a smaller number of the splicing points in this case. Including the IL of the pigtails spliced to the isolators (~0.2 dB) and splicing loss induced by the mismatch between the EDF and Flexcore fiber of WDMs (~0.2 dB), the total input

and output coupling losses are 1.53 dB and 1.54 dB, respectively. These results are important if one wants to determine the *intrinsic* performance of the EDFA in terms of noise figure and signal gain. Including the input and output coupling loss in the data, the results are treated as the ***system values*** and the system is referred to as a ***black box***.

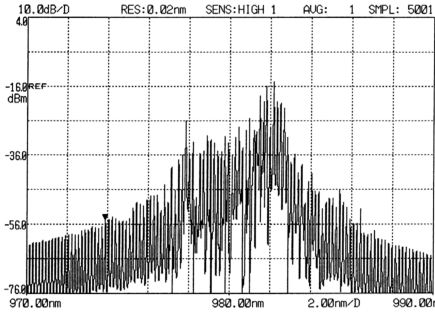

Fig. 3.2 *Spectral profile of 980 nm laser diode at the pump power of 89 mW monitored from 1% port of 980 nm coupler. The center wavelength is 980.2 nm and the 3–dB spectral width is 0.1 nm. Resolution was set at 0.02 nm.*

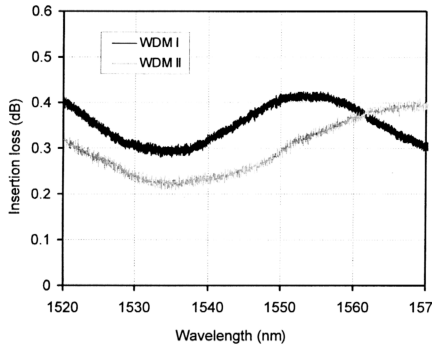

Fig. 3.3 *Insertion loss for the WDMs used in the setup.*

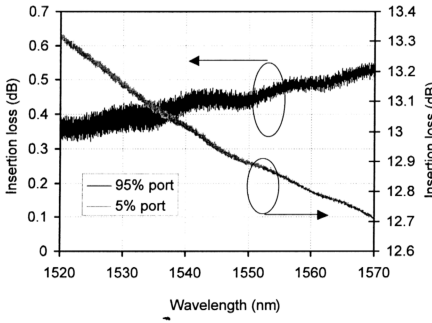

(a)

(continue...)

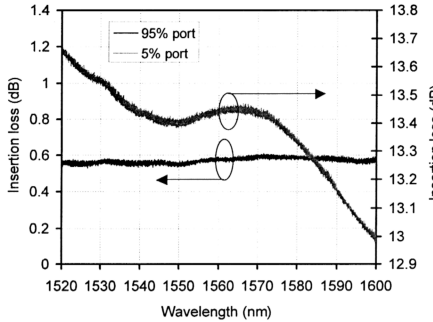

(b)

Fig. 3.4 *Insertion loss of 95 % and 5 % ports for (a) coupler C_1 and, (b) coupler C_2.*

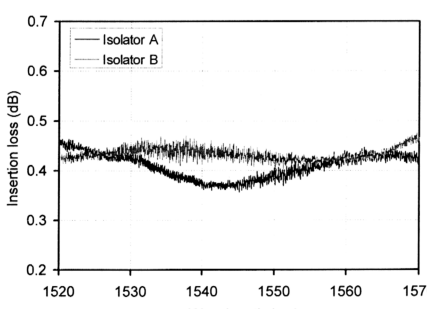

Fig. 3.5 *Insertion loss for isolators at the input and output ports of EDFA.*

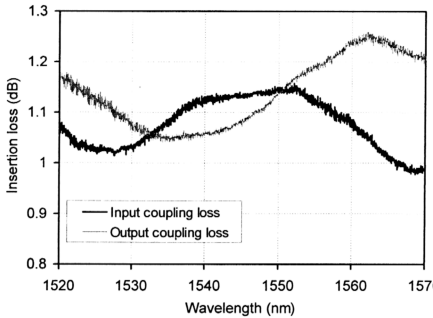

Fig. 3.6 *Insertion loss for input and output ports with all the components spliced together.*

3.3 STUDY OF BACK REFLECTION

In this section, back reflections from the coupler terminated port, spliced points and free fiber end are studied. The configuration shown in Fig. 3.7 was constructed. It is a part of the EDFA output as shown in Fig. 3.1. Note that fiber optic couplers are fabricated using two pieces optical fibers. In order to make a 1 X 2 fiber coupler, one of the ports has to be cut. Consequently, this terminated port becomes a source of the back reflection. A signal with an arbitrary wavelength of 1559 nm from a tunable laser source (TLS) was injected from the 5 % port and the back reflected signal was monitored using an optical spectrum analyzer (OSA) from the 95 % port. Fig. 3.8 shows the output power as a function of the input signal power for both cases with and without the index-matching gel at the free fiber end. Without the gel,

directivity of the coupler was < 40 dB. Both free fiber end and terminated port contribute to such a high reflection.

The coupler was then spliced to the system to form the configuration as shown in Fig. 3.9. In fact, this is the basic experimental setup that is being mentioned. Fig. 3.10 shows the back reflected signal power as a function of the input signal power with the pump turned OFF. In this case, the index-matching gel does not show any effect because the signal reaching at the free fiber end is very weak due to the strong absorption in the EDF. The reflected signal is further absorbed before reaching at the OSA. Note that the fiber splicing between the coupler C_2 and the WDM II markedly reduces the back reflection induced by the free fiber end in the configuration as shown in Fig. 3.7.

The pump is then turned on and the results for the pump power of 134.5 mW are shown in Fig. 3.11. The back reflected signal is now getting amplified. The free fiber end starts to contribute to such a high back reflection level. With the index-matching gel, the back reflected signal level has been reduced by ~10 dB. However, reflected signal level of ~-15 dBm with the gel at the input signal power of > –6 dBm is still considered high. Another source of the back reflection could be from the core size mismatch between EDF and the Flexcore fiber of WDMs. From the specification, the Flexcore fiber has a core diameter of 6 μm, 2.64 μm larger than that of the EDF used in the setup. The reflected signal is then amplified in the under-pumped EDF. It is worth noting that there is a maximum reflection level for each case after which the reflected level start to drop from the input signal power of ~5 dBm. The strong injected signal beyond –5 dBm, together with the strong back reflected signal, starts to saturate the active medium and results in a lower inversion level. In consequence,

the back reflected signal experiences a smaller amplification at the high input signal powers.

Injecting the signal in the port as shown in Figs. 3.7 and 3.9 is equivalent to the case of counter-feedback scheme as will be presented in Chapter 4. The reflected oscillating laser is thus still observed from the EDFA output port although the origin of the counter-feedback scheme is to eliminate the oscillating laser from the output port [1]. Same research work had been done to design an EDFA that is insensitive to the back reflection [2].

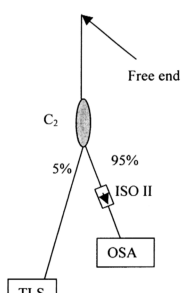

Fig. 3.7 *Simple configuration to study the back reflection from the coupler terminated port and free fiber end.*

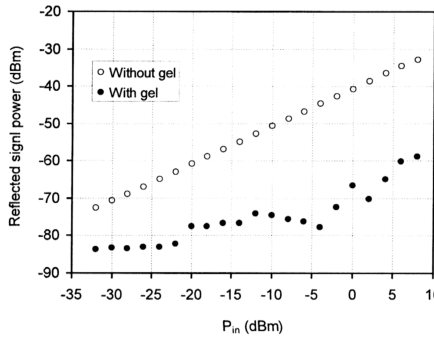

Fig. 3.8 *Back reflection from coupler C_1 as a function of input signal power at the signal wavelength of 1559 nm.*

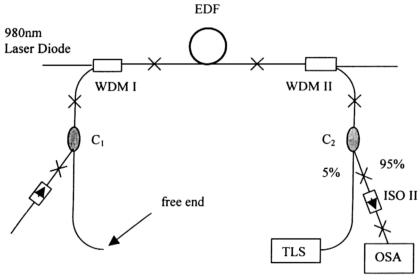

Fig. 3.9 *Basic experimental setup (as shown in Fig. 3.1) for back reflection study.*

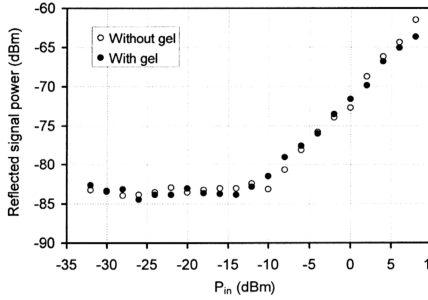

Fig. 3.10 *Back reflection for basic experimental setup as a function of input signal power at the signal wavelength of 1559 nm. The pump power is OFF.*

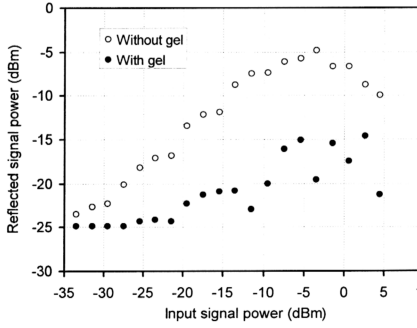

Fig. 3.11 *Back reflection for basic experimental setup as a function of input signal power at the signal wavelength of 1559 nm. The system is pumped at the power of 134.5 mW.*

3.4 SELECTION OF PUMPING SCHEME

In this section, selection of the pumping scheme is done based on a typical single-pass EDFA as shown in Fig. 3.1. The configuration shown in Fig. 3.1 is referred to as a co-pumping scheme where the pump source and the input signal are in the same direction. By changing the points A and B, the system becomes a counter-pumping scheme. In this scheme, the pump source is in the direction opposite that of the injected signal. In the previous studies [3], it has been shown that counter-pumping is able to achieve power conversion efficiency higher than that of the co-pumping scheme and thus a higher signal gain can be obtained.

Fig. 3.12 shows the forward ASE spectral profile for both co- and counter-pumping at the maximum pump power P_p = 134.5 mW. A higher power level is exhibited by the counter-pumping scheme since the output port is near to the input end of the pump source. However, if the pump power is high enough, or in other words, the EDF length is relatively short, the ASE spectrum becomes identical and the signal gain and the noise figure are very close to each other [4].

Fig. 3.13 shows the comparison of the signal gain and noise figure between both schemes at the small signal power P_{in} = –30 dBm. The signal wavelength was arbitrarily fixed at λ_{sig} = 1557.7 nm. Small discrepancy is obtained for the signal gain with the counter-pumping scheme achieves the gain by 1 dB higher than that of the co-pumping scheme at the maximum pump power P_p = 134.5 mW. Both systems start to become transparent to the input signal when P_p > 8.2 mW. For the available maximum pump power and the given EDF length, the maximum signal gains for the co- and counter-pumping schemes are 32.8 dB and 33.8 dB, respectively. If condition of near-complete inversion could be maintained along the fiber, the total gain experienced by the input signal would increase infinitely with the fiber length. But in

reality, four factors prevent such an unlimited signal growth [5]: 1) the pump power absorption with length, 2) the gain saturation by the amplified signal, 3) the gain saturation by the ASE and 4) the gain saturation by laser oscillation.

Although the signal gains are close to each other, the noise figure deviates markedly especially at the low pump powers as shown in Fig. 3.13. The deviation reduces to 2.2 dB at the maximum pump power. Note that for the counter-pumping scheme, the noise figure decreases with the pump power. At the low pump power, the noise figure is high (> 10 dB) since the pump power reaching at the EDF input end is less, resulting in a lower population at this input portion. By increasing the pump power, the population at the signal input end increases accordingly and thus a lower noise figure is achieved. The co-pumping scheme shows an opposite behavior where the noise figure increases with the pump power. In this scheme, the signal and the pump source enter the same EDF end where the backward ASE is strong. Such a backward ASE has a drawback in which it depletes the population (self-saturation) of the metastable level at the EDF input end. Note that the performance of the noise figure is dependent on the population at the EDF input end [5]. Therefore, the noise figure increases with the pump power since saturation effect is getting stronger with the pump power in this case. This is the case only for small input signal in the co-pumping scheme. For the high input signal powers, however, the noise figure decreases with the pump power. For example, with the input signal power of 0 dBm, the noise figure reduces from 10 dB at $P_p = 8.2$ mW to 6.3 dB at the maximum pump as shown in Fig, 3.14. As shown in Ref. [3, 6-9], the backward ASE can be suppressed by a certain level of the input signal. With the suppression of the backward ASE by the input signal power of 0 dBm, the noise figure can be improved

with the high pump powers. The signal- and laser-induced suppression of the backward ASE will be further treated in Chapters 4, 5 and 6.

Comparison between different pumping schemes as a function of input signal power at P_p = 58.7 mW and λ_{sig} = 1557.7 nm is shown in Fig. 3.15. The small signal gain is 30.8 dB for the co-pumping scheme and 30.2 dB for the counter-pumping scheme with the former scheme achieves the input saturation power of P_{in}^{sat} = –18 dBm, 3 dB lower than that of the latter. For the noise figure, the discrepancy between both schemes is > 3 dB. For the given available maximum pump power, the noise figure for the counter-pumping scheme is so high that is unacceptable in the practical application. In contrast, the noise figure for the co-pumping scheme is < 6 dB for the input signal power up to –2 dBm.

Although both schemes exhibit the signal gains that are very close to each other, the noise figure for the co-pumping scheme is much lower. Of course, a lower noise figure can be achieved in the counter-pumping scheme if a higher pump power is applied to the system since noise figure decreases with the pump power as shown in Fig. 3. 13. For the entire course of study, the co-pumping has been chosen.

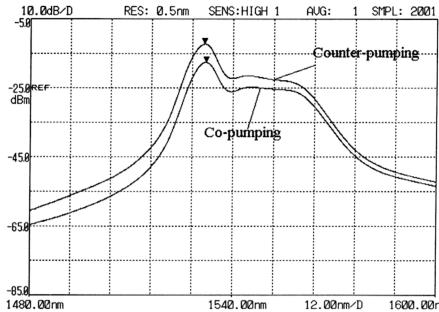

Fig. 3.12 *Forward ASE spectral profile for both co- and counter-pumping at the maximum pump power of 134.5 mW.*

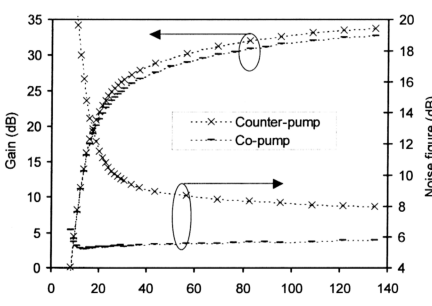

Fig. 3.13 *Comparison of the signal gain and noise figure between co- and counter-pumping schemes at the small signal power P_{in} = –30 dBm.*

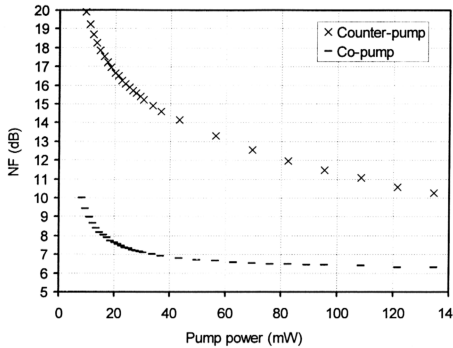

Fig. 3.14 *Comparison of the noise figure between co-and counter-pumping schemes at the high signal power of 0 dBm.*

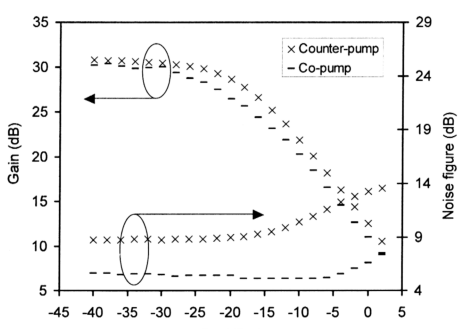

Fig. 3.15 *Comparison between co-and counter-pumping as a function of input signal power at the pump power of 58.7 mW and the wavelength λ_{sig} = 1557.7 nm.*

3.5 MEASUREMENT METHODS

3.5.1 Principle of Interpolation Method

EDFAs can be characterized with a stable laser source used as the input signal and an OSA for the spectral measurements. Spectral measurement of the laser source and the EDFA output are required to determine the EDFA parameters. The spectrum of the input signal shows that there is spontaneous emission coming from the laser source. This must be measured and accounted for in the calculation of the EDFA parameters.

The gain of the EDFA can be easily calculated as the difference between the input and output signal power as shown in Fig. 3.16. The input and output power levels measured are actually the sum of the signal power and the small amount of spontaneous emission power at the signal wavelength. It is negligible for low spontaneous emission levels. If the spontaneous emission level is high, it should be subtracted from each of the power measurement. In this case, the signal gain is determined by the following equation [9]:

$$G = \frac{P_{out} - P_{ASE}}{P_{in}} \tag{3.1}$$

where P_{out} = output signal power, P_{ASE} = spontaneous emission level at the signal wavelength, and P_{in} = input signal power.

The P_{ASE} is an important parameter in determining the noise figure which is given by [9]

$$NF = \frac{P_{ASE}}{Gh\nu\Delta\nu} + \frac{1}{G} \tag{3.2}$$

where $h\nu$ = photon energy for the input signal, and $\Delta\nu$ = bandwidth at P_{ASE} measurement. Ideally, an EDFA would amplify the input signal by its gain and

produce no additional output. However, the EDFA also produces ASE, which adds to the spontaneous emission produced by the source. In order to accurately determinate the noise figure, the P_{ASE} must be determined at the signal wavelength. However, it cannot be measured directly since the signal is superimposed on the spectrum of the ASE. Therefore, an approximate curve generated by *interpolation* is generally used to find the P_{ASE} as shown in Fig. 3.17. In the OSA (ANDO AQ6317B), various ways of fitting an interpolation curve are available such as Gaussian approximation, Lorentzian approximation, etc. It is important to select the most appropriate interpolation curve depending on the waveform.

3.5.2 Principles of Time-Domain-Extinction (TDE) Method [9-10]

The TDE method (Pulsed Method) take advantage of the fact that the metastable energy level of the erbium ion has a lifetime of ~10 ms. Immediately after the input signal is turned off, the ASE power remains at the same level it was in the presence of the input signal. Then it starts to rise in an exponential fashion until it reaches the level of an undriven condition.

In our study, an ANDO AQ8423Z Optical Amplifier Analyzer (OAA) was used to automatically control the measurement process. It utilizes 1 MHz modulation frequency, which is high enough to suppress a rise of ASE level during off signal. The OAA modulates signals from external light source with an acousto-optic modulator, AOM 1, and another modulator, AOM 2, selects the timing to measure signal or ASE level. When AOM 2 is set for ASE measurement, it eliminates the source signal and source spontaneous emission (SSE) without affecting the ASE level. Therefore, the OAA can measure the ASE at a signal wavelength very accurately. In this method, a signal whose intensity has been modulated by the AOM 1 is input to the EDFA. The

modulation frequency, 1 MHz, is a value sufficiently smaller than the lifetime of an Er^{3+} ion in the amplifier. Since the EDFA output signals are phase-isolated into the signal and the ASE light by switching ON/OFF of the AOM 1, it is possible to measure the signal, P_{out} and the ASE level independently by setting the phase of AOM 2 to each phase of the output signal as shown in Fig. 3.18.

The equations (3.1) and (3.2) are still applicable in calculating the signal gain and noise figure. Obviously, the difference between these two measurement methods is the way to determine the parameter of ASE level, P_{ASE}. In the TDE method, however, the isolation of the AOM 2 is not infinite. Consequently, if the input to the EDFA exceeds certain level, a leaked signal may appear on the measured waveform in the ASE measurement and causes errors in the signal gain and noise figure measurement.

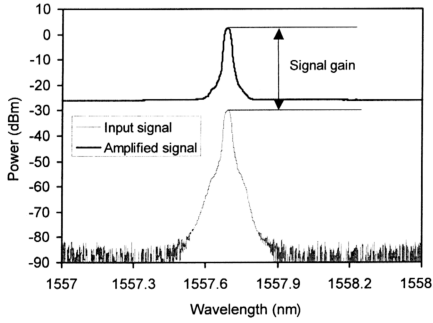

Fig. 3.16 *Signal gain determined by difference between the input and output signal power.*

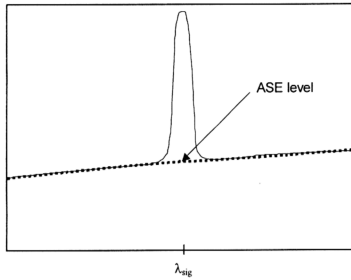

Fig. 3.17 *Interpolation method using curve fitting to determine the ASE level at signal wavelength.*

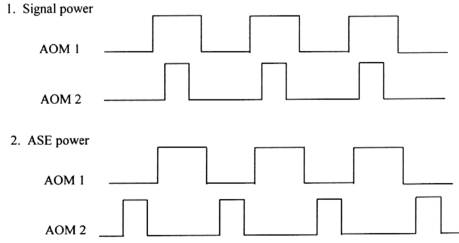

Fig. 3.18 *Timing diagram of the TDE*

3.5.3 Results Comparison between Different Measurement Methods

In this section, experimental comparison between the Interpolation Method and the TDE Method is done. The data is shown in Fig. 3.19. The input signal power was $P_{in} = -31.2$ dBm at the wavelength $\lambda_{sig} = 1550$ nm. The discrepancy of the signal gain between both measurement methods is fairly consistent with the interpolation method achieves the gain 0.4 dB higher than that obtained by the TDE method. For the noise figure the deviation is relatively large with the TDE method exhibits the noise figure ~0.7 dB higher for the entire pumping range.

Fig. 3.20 shows the signal gain and noise figure as a function of the input signal power at the pump power $P_p = 43.4$ mW and the signal wavelength $\lambda_{sig} = 1550$ nm. In the unsaturated regime, there is ~1 dB gain difference between both methods. However, the signal gains are found to be nearly identical at the saturated regime. The deviation is relatively large for noise figure with the TDE method achieves noise figure ~0.9 dB higher than that of the interpolation method. The results show that the interpolation method exhibits a high signal gain and a lower noise figure than that obtained using TDE method. The deviation is mostly arising from the different in the ASE level obtained using different measurement methods. In the interpolation method, the ASE level is measured at the wavelengths just above and just below the signal using an appropriate curve fitting. While the TDE method measures the ASE level by utilizing 1 MHz modulation frequency, which is high enough to suppress a rise of ASE level during the signal OFF phase. It is obviously that the TDE method measures the ASE level when the signal is OFF. Consequently, the ASE level measured using the latter method is higher, resulting in a lower signal gain and higher noise figure according to the Eqs. (3.1) and (3.2).

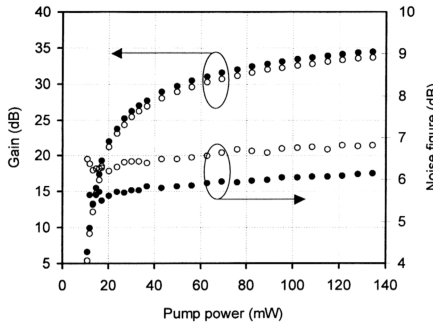

Fig. 3.19 *Signal gain and noise figure as a function of the pump power obtained from Interpolation Method and TDE Method. (o: TDE Method; •: Interpolation Method).*

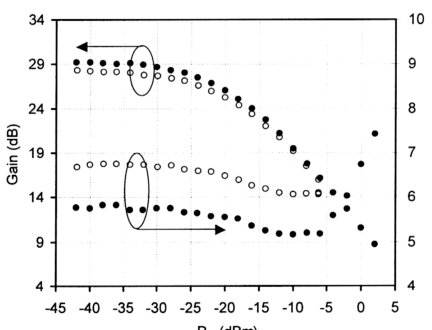

Fig. 3.20 *Signal gain and noise figure as a function of the input signal power at the pump power P_p = 43.4 mW and the signal wavelength λ_{sig} = 1550 nm. (o: TDE Method; •: Interpolation Method).*

3.6 STUDY OF BOOSTED SIGNAL SOURCE

In the TDE method, an OAA is used to automatically control the measurement process. However, the OAA introduces an insertion loss as high as ~8.5 dB. As a result, the maximum input signal power is only –6 dBm as shown in Fig. 3.20. In order to observe the saturation effect for the later studies, a higher input signal power is required. Thus, another EDFA is used as a booster to boost up the signal to be ~10 dBm. Considering the insertion loss introduced by the OAA, a final input signal power as high as ~2.5 dBm can be achieved. The boosted signal then consists of the amplified output power as well as the ASE that is not fully suppressed by the saturating signal from the TLS. This remaining ASE contributes to the degradation in the *signal-to-noise-ratio* (SNR) as compared to the signal monitored directly from the TLS without boosting. The output spectral for both types of signals is shown in Fig. 3.21.

Fig. 3.22 shows the SNR for both signals after amplification as a function of the input signal power P_{in} measured from the EDFA output. Without the booster, the SNR increases nearly linearly from the low input signal power to the input power of P_{in} ~22 dBm. In this small signal regime, contribution of the ASE from the EDFA-under-test degrades the SNR of the output signal. Above P_{in} > ~22 dBm, the ASE of the EDFA is efficiently suppressed. Therefore, SNR as high as ~56 dB is achieved for the input signal power beyond ~22 dBm. In contrast, the boosted signal shows a lower SNR. At the low P_{in}, the SNR deviation between both types of signals is relatively small since the ASE of the EDFA-under-test is not much affected by the small injection. A large deviation of ~10 dB at the high input signal power comes from the fact that the boosted signal itself consists of the ASE from the booster. This

ASE is getting amplified after passing through the EDFA-under-test and reduces the SNR of the boosted signal.

Since the boosted signal will be used for the later studies when the TDE method is applied, it is necessary to carry out the EDFA performance studies using this type of signal with the TDE method. Figs. 3.23, 3.24 and 3.25 show the signal gain and noise figure comparison between both types of signals as a function of pump power, input signal power and signal wavelength, respectively. The signal gains between both types of signals do not exhibit a significant deviation. For the noise figure, a deviation of ~0.3 dB is observed with the boosted signal exhibits a lower noise figure. Backward ASE suppression by a higher level of the ASE from the boosted signal is believed to be the mechanism that reduces the noise figure of the boosted signal. This mechanism is also observed in the later studies. Basically, deviation of ~0.3 dB in the noise figure is small. Therefore, the boosted signal is acceptable as a signal source for the studies.

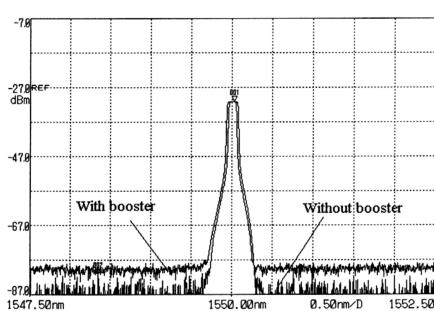

Fig. 3.21 *Output spectral for the signals with and without booster.*

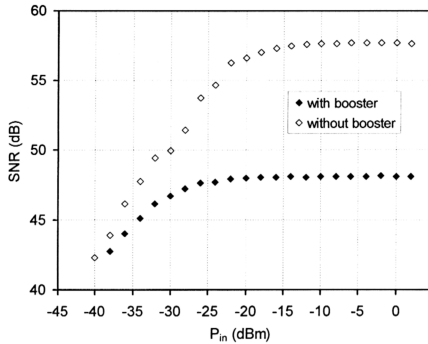

Fig. 3.22 *SNR for both signals after amplification as a function of the input signal power measured from the EDFA output.*

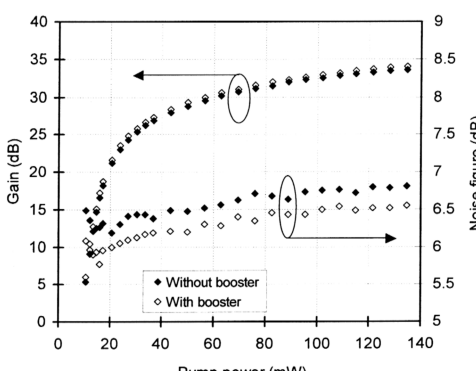

Fig. 3.23 *Signal gain and noise figure as a function of pump power at the input. signal power $P_{in} = -31.2$ dBm and the wavelength $\lambda_{sig} = 1550$ nm.*

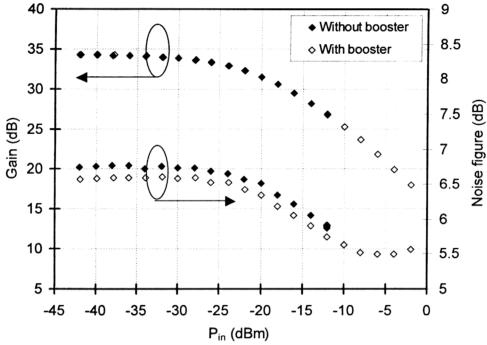

Fig. 3.23 *Signal gain and noise figure as a function of input signal power at the pump power P_p = 134.5 mW and the wavelength λ_{sig} = 1550 nm.*

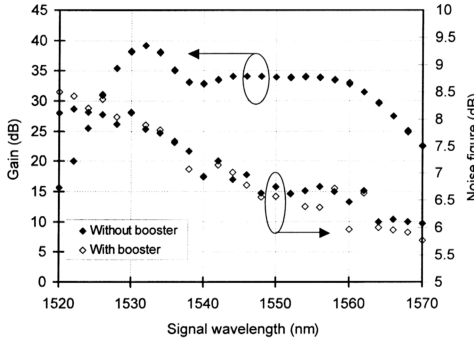

Fig. 3.23 *Signal gain and noise figure as a function of signal wavelength at the pump power P_p = 134.5 mW and the input signal power P_{in} = –31.2 dBm.*

3.7 CONCLUSIONS

Components used in the experimental setup have been well characterized in the wavelength range of study. The data showed that there was back reflection arising from both splicing points of the fibers and terminated ports of the fiber couplers. Study on different pumping schemes revealed that the counter-pumping scheme exhibited a relatively high noise figure (> 8 dB) where the co-pumping scheme achieved an acceptable noise figure (< 6 dB in the unsaturated regime). Discrepancy in signal gain was relatively small with the counter-pumping achieved ~0.6 dB higher. The co-pumping scheme has been chosen for the course of study due to its acceptable noise performance. Since Time-Domain-Extinction (TDE) Method will be applied in the later studies, evaluation has been done on this method. The noise figure measured by the TDE method was ~0.9 dB higher although the signal gain was ~1 dB lower. By boosting up the input signal to compensate the insertion loss (~8.5 dB) introduced by the Optical Amplifier Analyzer in the TDE method, noise figure was improved by ~0.3 dB. It was believed that the existence of the amplified spontaneous emission from the booster contributed to such an improvement of noise figure.

REFERENCES

[1] M. Kobayashi and S. Muro, "Gain stabilization in erbium-doped fiber amplifier with optical feedback loop using circulators," in OECC'98 Tech. Dig., pp. 98, 1998.

[2] C. Lester, K. Schusler, B. Pedersen, O. Lumholt, A. Bjarklev and J. H. Povlsen, "Reflection Insensitive Erbium-Doped Fiber Amplifier" IEEE Photon. Technol. Lett., 7, pp. 293, 1995.

[3] R. G. Smart, J. L. Zyskind, J. W. Sulhoff, and D. J. DiGiovanni, "An Investigation of the Noise Figure and Conversion Efficiency of 0.98 μm Pumped Erbium-Doped Fiber Amplifiers Under Saturated Conditions," IEEE Photon. Technol. Lett., 4, pp. 1261, 1992.

[4] Teyo Tuan Chin, "A Study of Gain-clamping and Injection Locking in Erbium-doped Fiber Amplifiers and Ring Lasers," M.Sc. Dissertation, 1999.

[5] E. Desurvire, Erbium-doped Fiber Amplifiers – Principles and Applications, John Wiley & Sons, Inc., 1994.

[6] Tuan Chin TEYO, Mun Kiat LEONG and Harith AHMAD, "Noise Characteristics of Erbium-doped Fiber Amplifier with Optical Counter-Feedback," Jpn. J. Appl. Phys., 41, Part 1, No. 5A, pp. 2949, 2002.

[7] T. C. Teyo, M. K. Leong and H. Ahmad, "Noise Characteristics of Erbium-doped Fiber Amplifier With Different Optical Feedback Schemes," Opt. Comm., 207, No. 1-6, pp. 327, 2002.

[8] T. C. Teyo, M. K. Leong and H. Ahmad, "Lasing wavelength dependence of gain clamped EDFA performance with different optical feedback schemes," accepted to be published in Opt. & Laser Technol.

[9] T. Nishikawa and T. Mori, "AQ8422/AQ8423A/AQ8423B Optical Amplifier Analyzer," Ando Technical Journal, pp. 39, July 1997.

[10] "EDFA Testing with the Time-Domain-Extinction Technique," HP Product Note 71452.2.